DEVELOPMENTAL DYNAMICS 243:1487–1498, 2014
DOI: 10.1002/DVDY.24186

The Role of *Zic* Genes in Inner Ear Development in the Mouse: Exploring Mutant Mouse Phenotypes

Andrew P. Chervenak,[1,2] Lisa M. Bank,[1] Nicole Thomsen,[3] Hannah C. Glanville-Jones,[3] Jonathan Skibo,[4] Kathleen J. Millen,[4] Ruth M. Arkell,[3] and Kate F. Barald[1,2,5]*

[1]Department of Cell and Developmental Biology, University of Michigan Medical School, Ann Arbor, Michigan
[2]Cellular and Molecular Biology Graduate Program, University of Michigan Medical School, Ann Arbor, Michigan
[3]Early Mammalian Development Laboratory Research School of Biology, The Australian National University, Canberra, Australia
[4]Seattle Children's Research Institute, Center for Integrative Brain Research, Seattle, Washington
[5]Department of Biomedical Engineering, College of Engineering, University of Michigan, Ann Arbor, Michigan

Background: Murine *Zic* genes (*Zic1–5*) are expressed in the dorsal hindbrain and in periotic mesenchyme (POM) adjacent to the developing inner ear. *Zic* genes are involved in developmental signaling pathways in many organ systems, including the ear, although their exact roles haven't been fully elucidated. This report examines the role of *Zic1*, *Zic2*, and *Zic4* during inner ear development in mouse mutants in which these *Zic* genes are affected. Results: *Zic1*/*Zic4* double mutants don't exhibit any apparent defects in inner ear morphology. By contrast, inner ears from *Zic2*$^{kd/kd}$ and *Zic2*$^{Ku/Ku}$ mutants have severe but variable morphological defects in endolymphatic duct/sac and semicircular canal formation and in cochlear extension in the inner ear. Analysis of otocyst patterning in the *Zic2*$^{Ku/Ku}$ mutants by in situ hybridization showed changes in the expression patterns of *Gbx2* and *Pax2*. Conclusions: The experiments provide the first genetic evidence that the *Zic* genes are required for morphogenesis of the inner ear. *Zic2* loss-of-function doesn't prevent initial otocyst patterning but leads to molecular abnormalities concomitant with morphogenesis of the endolymphatic duct. Functional hearing deficits often accompany inner ear dysmorphologies, making *Zic2* a novel candidate gene for ongoing efforts to identify the genetic basis of human hearing loss. *Developmental Dynamics 243:1487–1498, 2014*. © 2014 Wiley Periodicals, Inc.

Key words: Zic1; Zic2; Zic4; inner ear; embryogenesis; mouse

Submitted 1 March 2014; First Decision 23 July 2014; Accepted 25 August 2014; Published online 1 September 2014

Introduction

The *Zic* genes encode a family of zinc finger–containing transcription factors. The zinc finger domain is known to participate in both DNA binding and protein binding, enabling ZIC proteins to participate in a range of interactions (reviewed in Ali et al. 2012; Houtmeyers et al., 2013). For example, ZIC proteins can act as classical transcription factors to bind DNA and control transcription (Aruga et al., 1994; Yang et al., 2000; Salero et al., 2001; Ebert et al., 2003; Mizugishi et al., 2004; Sakurada et al., 2005; Lim et al., 2010) or they can act as co-factors to bind other proteins and influence gene transcription without themselves contacting DNA (Koyabu et al., 2001; Mizugishi et al., 2001; Pan et al., 2011; Pourebrahim et al., 2011). The vertebrate ZIC proteins are generally encoded by five genes at three genomic locations. *Zic1* and *Zic4* exist as a divergently transcribed tandem gene pair, as do *Zic2* and *Zic5*, while *Zic3* exists as a singleton (Houtmeyers et al., 2013).

Each of the gene pairs appears to share some regulatory elements, such that *Zic1* and *Zic4* have highly overlapping mRNA expression patterns as do *Zic2* and *Zic5* (Houtmeyers et al., 2013). Furthermore, in some cases the expression of all five *Zic* genes overlaps, such as during inner ear development in both mouse and chick (Chervenak et al., 2013), raising the possibility that the *Zic* genes could act redundantly during development. Mutation of individual *Zic* genes does, however, produce exclusive phenotypes indicating partial functional divergence (Grinberg and Millen, 2005; Houtmeyers et al., 2013). The multifunctional nature of the ZIC proteins enables them to act in a wide range of processes as demonstrated by the pleiotropic nature of *Zic* mutant phenotypes (Grinberg and Millen, 2005; Houtmeyers et al., 2013).

Because of the redundant and multifunctional features of *Zic* activity, the use of phenotype analysis to infer the mechanisms of *Zic* gene function is difficult. Despite the long-term availability of *Zic* mouse mutants and a growing list of *Zic*-dependent

Grant sponsor: National Institutes of Health/National Institute on Deafness and Other Communication Disorders; Grant number: 2 RO1 DC04184; Grant sponsor: National Institutes of Health/National Institute of General Medical Sciences: Cellular and Molecular Biology; Grant number: T32-GM007315; Grant sponsor: National Institutes of Health/National Institute of Diabetes, Digestive and Kidney Disease; Regenerative Sciences; Grant number: 5T90DK070071-05; Grant sponsor: National Institutes of Health/National Institute on Deafness and Other Communication Disorders; Hearing, Balance, and Chemical Senses; Grant number: 5T32DC000011-32.
*Correspondence to: Kate F. Barald, Department of Cell and Developmental Biology, Department of Biomedical Engineering 3053 BSRB, 109 Zina Pitcher Place, Ann Arbor, MI 48109-2200. E-mail: kfbarald@umich.edu

Article is online at: http://onlinelibrary.wiley.com/doi/10.1002/dvdy.24186/abstract

biological processes (Houtmeyers et al., 2013), the molecular basis of *Zic* requirements is generally unknown and it is likely that further *Zic*-dependent processes remain to be discovered. To determine whether the *Zic* genes may be involved in inner ear development, we recently characterized the expression of *Zic1–5* (mouse) and *Zic1–4* (chick) in the region of the developing inner ear of chick and mouse embryos (Chervenak et al., 2013). Each of the *Zic* genes is expressed in the dorsal hindbrain and periotic mesenchyme (POM) adjacent to the developing inner ear, but not in the developing otic epithelium, in either mouse or chick embryos. Similar to findings for other regions where the *Zic* genes are expressed (Elms et al., 2004), each *Zic* gene has a unique spatiotemporal expression pattern during inner ear development, but the spatio-temporal expression of any individual *Zic* gene partially overlaps with another/others (Chervenak et al., 2013). Moreover, the *Zic* genes have been proposed to interact with the SHH, BMP, and WNT signaling pathways (Rohr et al., 1999; Nyholm et al., 2007), each of which is implicated in otic vesicle development. The *Zic* genes may function with the neuroepithelium itself to control the production of the otic vesicle patterning signals, or within the POM to relay signals from one or more of the neuroepithelial-derived pathways. Alternatively, they may participate in the mesenchymal-epithelial signaling required for the development of the inner ear.

In this study, we used phenotype analysis to determine which, if any, of the murine *Zic* genes play a non-redundant role during inner ear development. The inner ears from animals homozygous null for the *Zic1*/*Zic4* gene pair (Grinberg et al., 2004; Blank et al., 2011) were examined and found to be indistinguishable from those of wild type animals at all stages examined between E11.5 and E15.5. In contrast, the inner ears from either of two different mutant alleles of *Zic2* (Nagai et al., 2000; Elms et al., 2003) exhibited a variety of structural defects, including loss of the endolymphatic duct and sac, and loss of, truncation of, or morphological malformation of the semicircular canals and cochlear duct. In addition, the size of the otocyst and resulting inner ears was much smaller than that in wild type littermates. Molecular analysis revealed that initial patterning of the otocyst (at E9.5) occurs as expected but abnormalities in the level and/or distribution of key transcription factors is perturbed from E10.5 onwards.

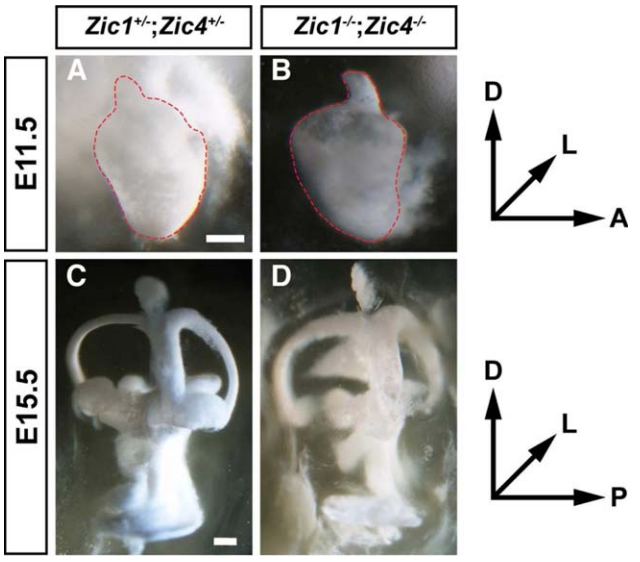

Fig. 1. Morphology of inner ears from *Zic1*/*Zic4* mice. Ears from *Zic1*$^{+/-}$;*Zic4*$^{+/-}$ (**A, C**) and *Zic1*$^{-/-}$;*Zic4*$^{-/-}$ (**B, D**) mice were paint-filled at E11.5 (A,B) and E15.5 (C, D) to look for changes in inner ear morphology. D, dorsal; L, lateral; A, anterior; P, posterior. Scale bar in A = 100 μm (applies to A, B); scale bar in C = 200 μm (applies to C, D).

Results

Morphological Analysis of Inner Ears from *Zic* Mutant Mice

Murine Zic1 and Zic4 are not required for inner ear development

Ears from *Zic1*$^{+/-}$; *Zic4*$^{+/-}$ and *Zic1*$^{-/-}$; *Zic4*$^{-/-}$ mouse embryos at E11.5 (Fig. 1A, B) and E15.5 (Fig. 1C, D) were paint-filled to examine changes in inner ear morphology. The combined loss of *Zic1* and *Zic4* had no noticeable effect on the structures of the inner ear at the times examined (E11.5 and E15.5; compare Fig. 1B and A, 1D and C).

Partial loss-of-Zic2 is sufficient to impair inner ear development.

The *Zic2*^{kd} allele (*Zic2*^{tm1Jaru}, MGI: 2156825), generated by homologous recombination, expresses a decreased level of the wild-type *Zic2* transcript and protein. Homozygotes die prenatally and exhibit variable spine bifida and anencephaly (Nagai et al., 2000). Heterozygotes are viable and fertile. To determine whether Zic2 function is required for inner ear development, paint-filled inner ears from *Zic2*$^{+/+}$, *Zic2*$^{+/kd}$, and *Zic2*$^{kd/kd}$ embryos were compared at E11.5, E13.5, E16.5, and E18.5 (Fig. 2). At E11.5 when the endolymphatic duct normally begins to emerge from the dorsal surface of the otocyst and the cochlear duct emerges ventrally, no morphological differences were detected in the inner ears of *Zic2*$^{kd/kd}$ embryos (compare Fig. 2A and B). The inner ear undergoes further morphological changes, including the formation of the semicircular canals and the emergence and coiling of the cochlea, and by E13.5, the inner ear has assumed its distinctive three-dimensional shape. Wild type (Fig. 2C) and heterozygous (Fig. 2D) embryos have inner ears that contain all structures, including the three semicircular canals (anterior, lateral, and posterior), the endolymphatic sac, cochlea, saccule, and the utricle, which cannot be seen in this view of the ears. In contrast, the inner ears from *Zic2*$^{kd/kd}$ embryos (Fig. 2E) lack the endolymphatic duct/sac, have missing or incomplete semicircular canals, and have a cochlea that initially grows dorsally rather than anteriorly (compare Fig. 2E and C, D). Further refinements to the inner ear structures occur by E16.5, including outgrowth and coiling of the cochlea, and these changes are evident in the wild type inner ear (Fig. 2F). In comparison, the inner ears from *Zic2*$^{kd/kd}$ embryos have an indeterminate shape, with a failure of most of the structures to develop, though a partial semicircular canal has formed in the embryo pictured, as has a rudiment of the cochlea (Fig. 2G). Comparisons of the inner ears from the *Zic2*$^{kd/kd}$ embryos at E13.5 (Fig. 2E) and E16.5 (Fig. 2G) show variability in the severity of the inner ear phenotype. At E18.5, in the wild type inner ear. the cochlea has coiled further (Fig. 2H). Inner ears from *Zic2*$^{kd/kd}$ embryos again show a variability in the severity of the phenotype, with some ears only missing one semicircular canal and having a slightly deformed cochlea (Fig. 2I),

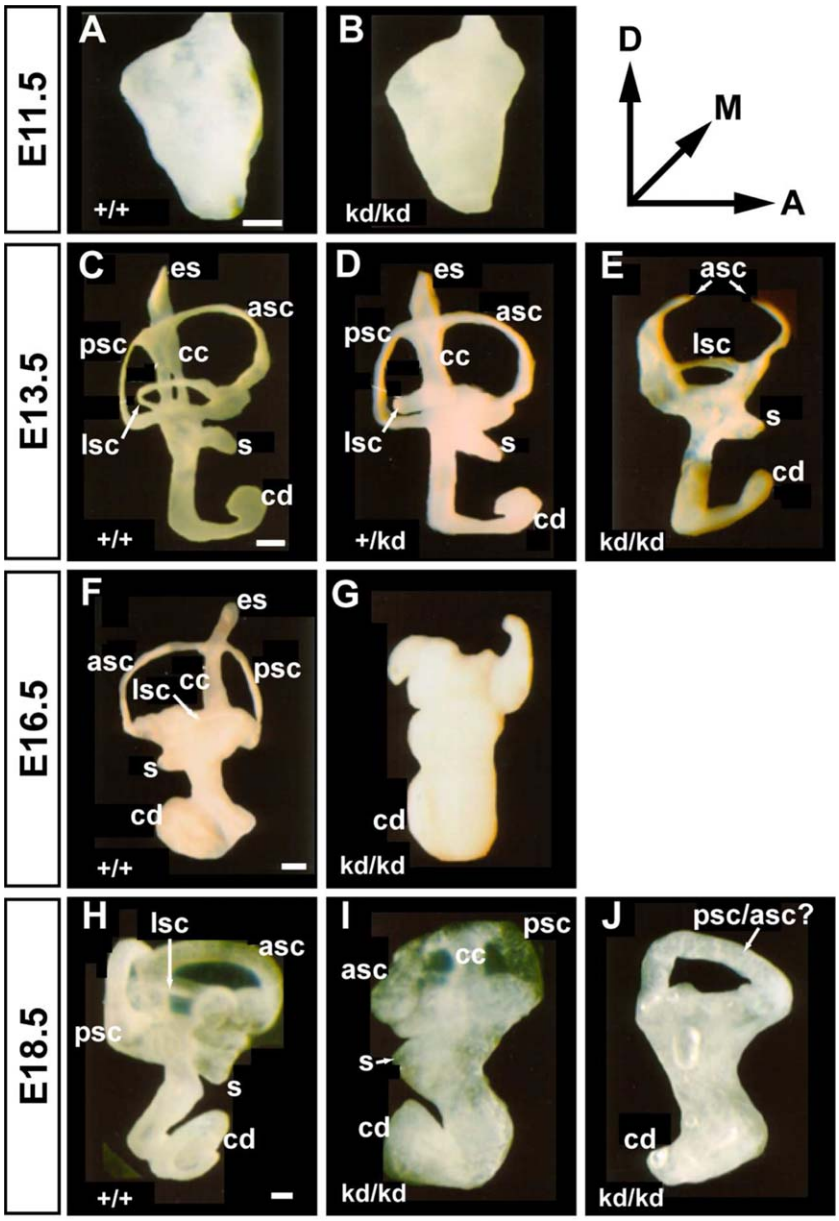

Fig. 2. Reduced levels of *Zic2* result in severe inner ear morphological defects. Ears from $Zic2^{+/+}$ (**A, C, F, H**), $Zic2^{+/kd}$ (**D**), and $Zic2^{kd/kd}$ (**B, E, G, I, J**) embryos were paint-filled at E11.5 (A,B), E13.5 (C–E), E16.5 (F, G), and E18.5 (H–J) to look for changes in inner ear morphology. At E18.5, the ducts appear thicker due to a perilymphatic rather than endolymphatic-only fill (Kiernan 2006). D, dorsal; M, medial; A, anterior; es, endolymphatic sac; cc, common crus; asc, anterior semicircular canal; psc, posterior semicircular canal; lsc, lateral semicircular canal; s, saccule; cd, cochlear duct. Scale bar in A = 100 μm (applies to A, B); scale bar in C = 200 μm (applies to C–E); scale bar in F = 200 μm (applies to F, G); scale bar in H = 200 μm (applies to H–J).

while others are missing multiple semicircular canals and the saccule and have a more severely affected cochlea (Fig. 2J).

Severe loss of Zic2 function further impairs inner ear development.

To corroborate this finding, the inner ears from a more severe *Zic2* allele ($Zic2^{Ku}$, MGI: 1862004) were also examined. This chemically induced allele encodes a Zic2 protein that is unable to bind DNA due to a missense mutation that alters a canonical residue in the 4th zinc finger (Elms et al., 2003; Brown et al., 2005). Embryos homozygous for this allele die at mid-gestation (Elms et al., 2003) and display classical holoprosencephaly (Warr et al., 2008) and laterality defects (Barratt et al., 2014), indicating that it is a more severe allele than $Zic2^{kd}$. Inner ears from $Zic2^{+/+}$, $Zic2^{Ku/+}$, and $Zic2^{Ku/Ku}$ embryos were also paint-filled at E11.5 and E12.5 to look for changes in inner ear morphology (Fig. 3). At E11.5, the gross morphology of inner ears from heterozygotes (Fig. 3B) appeared identical to those from wild type embryos (Fig. 3A). Inner ears from $Zic2^{Ku/Ku}$ mutants, however, were noticeably smaller and had truncated endolymphatic ducts and cochleae compared to either wild type or heterozygous littermates (compare Fig. 3C and A, B). To quantify the size differences observed in the $Zic2^{Ku/Ku}$ inner ears, we measured and compared the

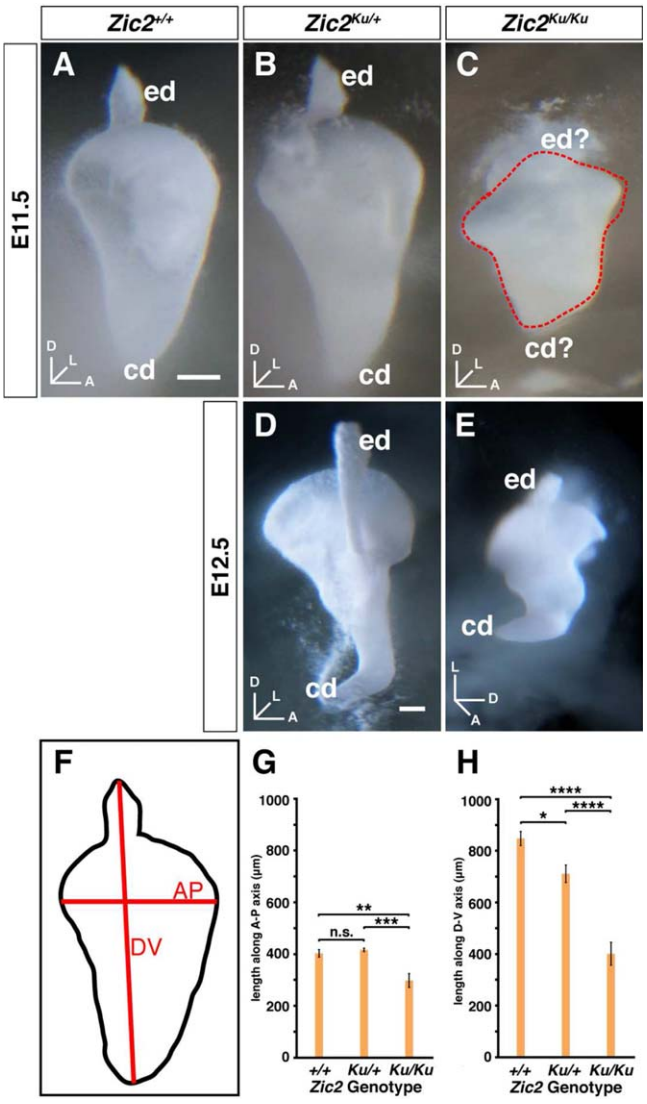

Fig. 3. Analysis of inner ear morphology from *Zic2*$^{Ku/Ku}$ mice. Inner ears from *Zic2*$^{+/+}$ (**A**), *Zic2*$^{Ku/+}$ (**B, D**), and *Zic2*$^{Ku/Ku}$ (**C, E**) mouse embryos at E11.5 (A–C) and E12.5 (D, E) were paint-filled to assess changes in gross morphology. Measurements were taken along the anterior-posterior and dorsal-ventral axes of inner ears at E11.5 as shown in **F** and compared among the three genotypes. Comparison of ear dimensions along the anterior-posterior (**G**) and dorsal-ventral (**H**) axes. values are designated in the figure as follows: **P*<0.05; ***P*<0.05; ***p<0.005; *****P*<0.0001; n.s., not significant. Error bars in G and H represent the SEM. D, dorsal; L, lateral; A, anterior; AP, anterior-posterior; DV, dorsal-ventral; ed, endolymphatic duct; cd, cochlear duct. Scale bar in A = 100 μm (applies to A–C); scale bar in D = 100 μm (applies to D–E).

length and width of the inner ears from *Zic2*$^{+/+}$, *Zic2*$^{Ku/+}$, and *Zic2*$^{Ku/Ku}$ embryos (Fig. 3F–H). *Zic2*$^{Ku/Ku}$ inner ears were significantly shorter along both axes when compared to *Zic2*$^{+/+}$ and *Zic2*$^{Ku/+}$ littermates (Fig. 3G, H). In addition, *Zic2*$^{Ku/+}$ ears were significantly shorter (relative to wild type) along their dorsal-ventral (but not anterior-posterior) axis (Fig. 3G, H).

By E12.5, inner ears from *Zic2*$^{Ku/Ku}$ mutants appeared to be even smaller compared to those from heterozygotes, but the heterozygote mutant ears had roughly the same morphological features as those seen in the wild type inner ear (see Fig. 3D). In addition, inner ears from the *Zic2*$^{Ku/Ku}$ mutants were rotated ~90°, such that any evidence of an emerging rudimentary endolymphatic duct pointed laterally instead of dorsally (Fig. 3E). At E12.5, the *Zic2*$^{Ku/Ku}$ mutants are close to death and a large proportion of the recovered embryos are in an advanced state of necrosis making them unsuitable for histological analysis. This led to a small sample size at E12.5 preventing quantification of otocyst size. The mid-gestation lethality also precluded the analysis of inner ear morphology at later time-points. The severe morphological defects of the developing ear in *Zic2*$^{Ku/Ku}$ embryos suggest they may be a good model for characterization of the molecular mechanism(s) underlying the observed phenotype and these embryos were chosen for further analysis.

Gross Morphology of *Zic2*$^{Ku/Ku}$ Mid-gestation Embryos

The nervous system of *Zic2*$^{Ku/Ku}$ embryos is profoundly affected such that, as previously described, by E9.5, the embryos exhibit neural tube closure defects, forebrain haematomas, and a "kinked" neural tube throughout the trunk of these embryos (Elms et al., 2003). This study did not document later neurectoderm phenotypes nor the location and gross morphology of the developing inner ear. We therefore examined these aspects of the *Zic2*$^{Ku/Ku}$ phenotype. At E9.5, the *Zic2*$^{Ku/Ku}$ mutants are easily distinguished from their wild type and heterozygous littermates due to large regions of the neural tube that fail to close (arrowheads in Fig. 4C). The overall size of the *Zic2*$^{Ku/Ku}$ mutants, however, is not noticeably different from that of their *Zic2*$^{+/+}$ or *Zic2*$^{Ku/+}$ littermates (compare Fig. 4C and A, B). Similarly, the overall size and shape of the otocyst in *Zic2*$^{Ku/Ku}$ mutants are indistinguishable from that of wild type or heterozygous littermates (compare Fig. 4C' and A', B'). In *kumba* mutants, in which the neural tube fails to close properly in the region of the hindbrain, the distance between the otocysts was greater than in *Zic2*$^{+/+}$ and *Zic2*$^{Ku/+}$ littermates (compare Fig. 4C'' and A'', B''). *Zic2*$^{Ku/Ku}$ mutants also displayed exencephaly in the midbrain (Fig. 4D), malformation of the forebrain, including hematomas (yellow arrows in Fig. 4D'), and a kinked neural tube in the trunk region of the embryo (Fig. 4D'').

As development progresses, the *Zic2*$^{Ku/Ku}$ mutants can be further distinguished from their wild type and heterozygous littermates. At E11.5, *Zic2*$^{Ku/Ku}$ mutants are visibly smaller than *Zic2*$^{+/+}$ and *Zic2*$^{Ku/+}$ embryos (compare Fig. 5C and A, B). In addition, all mutants have an open neural tube (arrowheads in Fig. 5C. An enlarged view of the caudal neural tube defect is seen in Fig. 5C', an enlarged view of exencephaly in the hindbrain is depicted in Fig. 5C'') and some embryos display a kinked or bent tail (asterisk in Fig. 5C). To quantify the size difference between the mutants and their littermates, we measured along the neural tube from the middle of the otocyst to the middle of the forelimb and compared these distances among the three genotypes (schematic in Fig. 5D). The *Zic2*$^{Ku/Ku}$ mutants had a significantly shorter otocyst-to-forelimb distance compared to either wild type or heterozygous littermates (Fig. 5E). We found no difference in somite numbers among the *Zic2*$^{+/+}$, *Zic2*$^{Ku/+}$, or *Zic2*$^{Ku/Ku}$ embryos, indicating that the shortened otocyst-to-forelimb distance was not due to defects in somitogenesis. Instead, the shortened distance likely results from defects in the specification of segments along the neural tube. Consistent with this explanation, previous work found that rhombomeres 3 and 5 were smaller in the *Zic2*$^{Ku/Ku}$ mutants at E9.5, which may at least partially

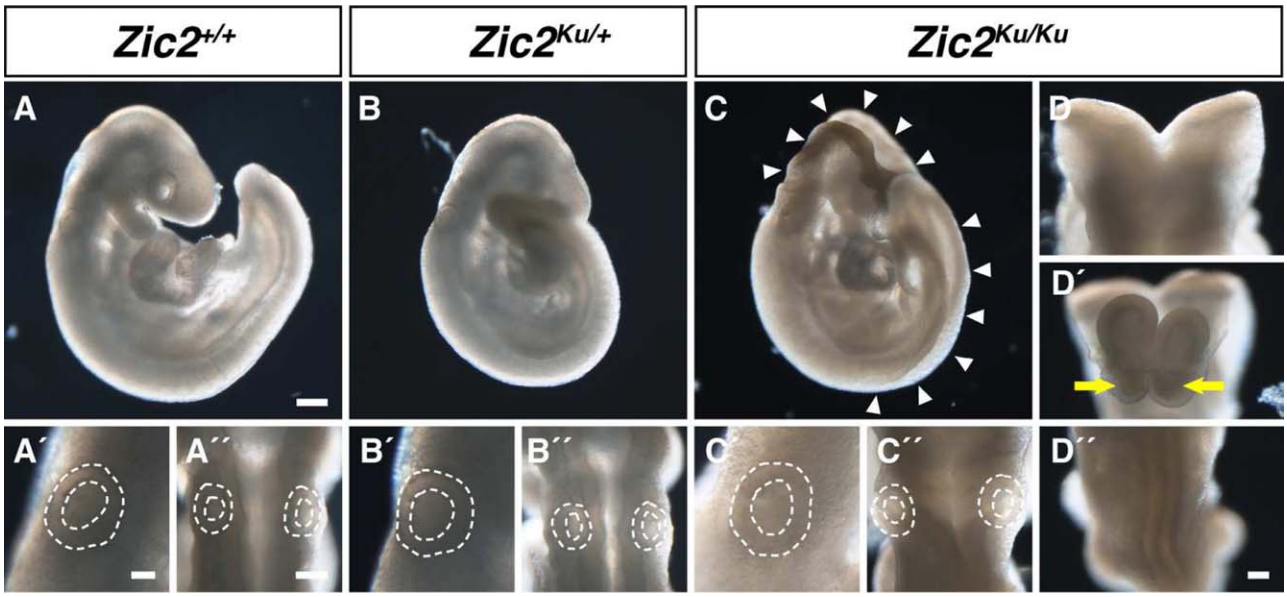

Fig. 4. Gross morphology of *Zic2*^{kumba} embryos at E9.5. *Zic2*$^{+/+}$ (**A–A"**) and *Zic2*$^{Ku/+}$ (**B–B"**) embryos show no gross morphological defects at E9.5. *Zic2*$^{Ku/Ku}$ embryos (**C–C", D–D"**) have severe defects in the forebrain, midbrain, hindbrain, and caudal regions of the neural tube (arrowheads in C). Higher magnification images show exencephaly in the midbrain (D), malformation of the forebrain, including hematomas (D'; yellow arrows indicate hematomas), and a kinked neural tube in the trunk region of the embryo (D"). The otocysts appear to be normal in size and shape in *Zic2*$^{+/+}$ (A'), *Zic2*$^{Ku/+}$ (B'), and *Zic2*$^{Ku/Ku}$ (C') embryos. However, the paired otocysts from *Zic2*$^{+/+}$ (A") and *Zic2*$^{Ku/+}$ (B") embryos are located near the midline, while otocysts from *Zic2*$^{Ku/Ku}$ embryos (C") are located farther away from the midline due to the failure of the neural tube to close. White dashed lines outline the otocysts. Scale bar in A = 200 μm (applies to A–C); scale bar in A' = 50 μm (applies to panels A'–C'); scale bar in A" = 100 μm (applies to A"–C"); scale bar in D" = 100 μm (applies to D–D").

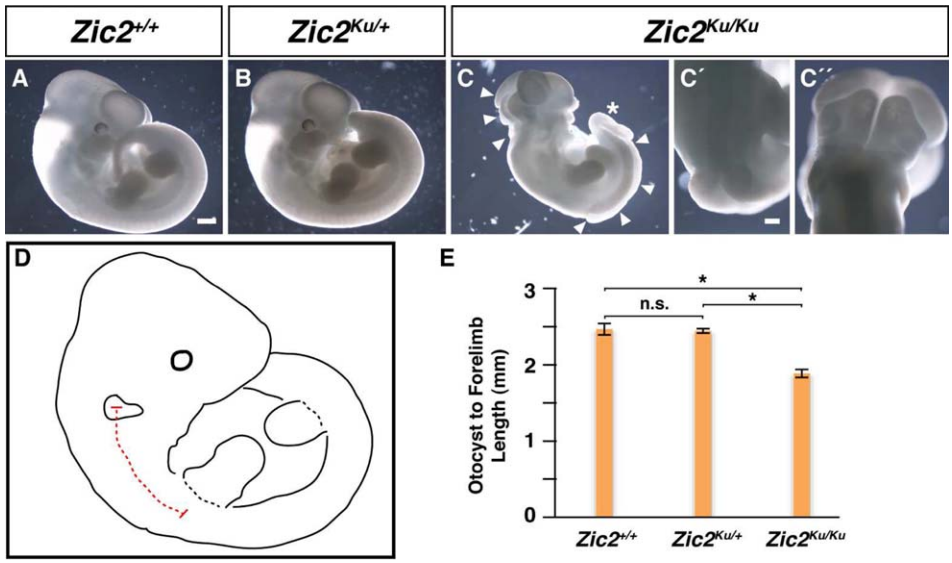

Fig. 5. Gross morphology of *Zic2*^{kumba} embryos at E11.5. Although *Zic2*$^{+/+}$ (**A**) and *Zic2*$^{Ku/+}$ (**B**) embryos show no gross morphological defects at E11.5, the *Zic2*$^{Ku/Ku}$ embryos (**C-C"**) are smaller than both their *Zic2*$^{+/+}$ and *Zic2*$^{Ku/+}$ littermates, have severe defects in the hindbrain and caudal regions of the neural tube (arrowheads in C), and display a kinked tail (asterisk in C). Higher magnification images show failure of the caudal neural tube to close (C') and exencephaly in the hindbrain (C"). The trunk length of the embryos from the midpoint of the otocyst to the midpoint of the forelimb was measured as shown in **D** and compared among the three genotypes (**E**; n=6 for each genotype). p-values are designated as follows: *$P<0.0001$; n.s., not significant. Error bars in E represent the SEM. Scale bar in A = 500 μm (applies to panels A–C); scale bar in C' = 200 μm (applies to C'–C").

explain the shortened otocyst-to-forelimb distance (Elms et al., 2003).

One day later at E12.5 (Fig. 6), the accumulated neural tube closure defects cause the *kumba* mutants to look very different from either the *Zic2*$^{+/+}$ or *Zic2*$^{Ku/+}$ embryos. *Zic2*$^{Ku/Ku}$ embryos are smaller than their littermates and have open neural tubes in both caudal and rostral regions (compare Fig. 6C and A, B; arrowheads in Fig. 6C denote regions of open neural tube). At

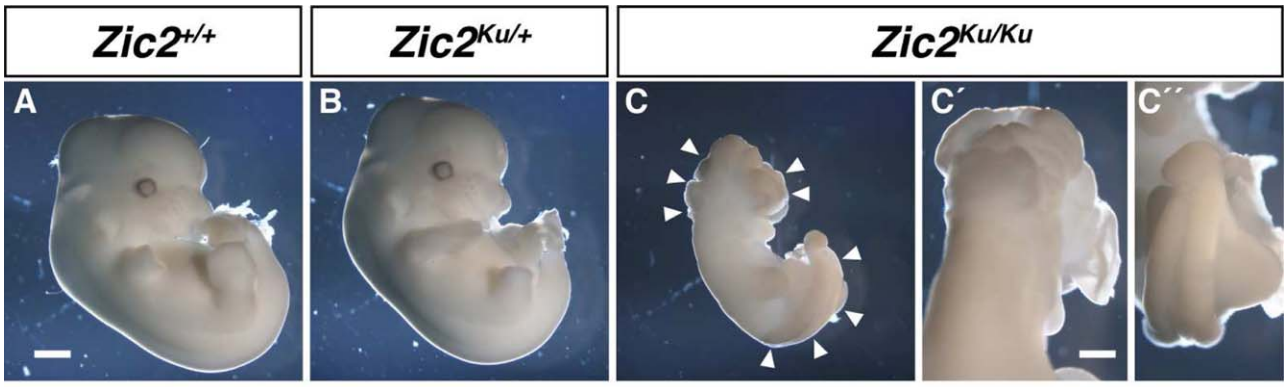

Fig. 6. Gross morphology of *Zic2*^{kumba} embryos at E12.5. *Zic2*$^{+/+}$ (**A**) and *Zic2*$^{Ku/+}$ (**B**) embryos show no gross morphological defects at E12.5. However, *Zic2*$^{Ku/Ku}$ embryos (**C–C"**) are smaller than both their *Zic2*$^{+/+}$ and *Zic2*$^{Ku/+}$ littermates and have severe defects in the forebrain, hindbrain, and caudal regions of the neural tube (arrowheads in C). Higher magnification images show exencephaly in the hindbrain (C') and spina bifida in the caudal neural tube (C"). Scale bar in A = 1,000 μm (applies to A–C); scale bar in C' = 500 μm (applies to C'–C").

higher magnifications, exencephaly in the hindbrain (Fig. 6C'), spina bifida in the caudal neural tube (Fig. 6C''), and a kinked tip of the tail (Fig. 6C'') can be seen more clearly.

**Altered Positioning of the Otocyst Relative to the Hindbrain in *Zic2*$^{Ku/Ku}$ Mutants

The location and position of the otocyst were examined in embryos at all stages (E9.5 to E12.5) and ears from the *Zic2*$^{Ku/Ku}$ mice were found to be abnormally positioned relative to the neural tube. The precise nature of the positional abnormalities varied between mutants (Fig. 7A), but included: tilting of the ears so that the dorsal-ventral axis of the otocyst was now oriented in a dorso-lateral to ventro-medial direction (TILTED); curling of the open neural tube around the upper portion of the otocyst (CURL-OVER); an increase in the distance between the otic epithelium and the neural tube (SEPARATED); and abnormally shaped otocysts (ALTERED SHAPE). The neural tube closure defects also varied and could be classified into distinct types (Fig. 7B), including open neural tube (Type I), open neural tube that curled (Type II), and neural tube that improperly closed (Type III).

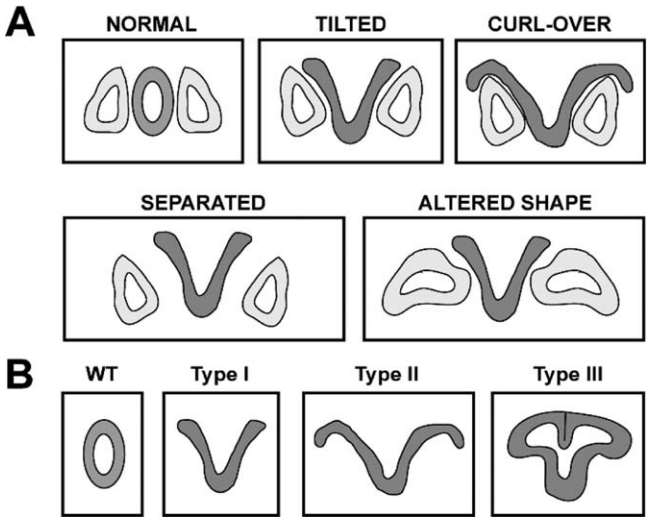

Fig. 7. Variability of the inner ear phenotypes in *Zic2*$^{Ku/Ku}$ mice. **A:** Variations observed in the shape and position of the otocyst relative to the neural tube in the *Zic2*$^{Ku/Ku}$ mutants. **B:** Variations observed in the extent of neural tube closure defects in the *Zic2*$^{Ku/Ku}$ mutants.

In Contrast to Effects on the Inner Ear, Otocyst Patterning Is Unaffected in the *Zic2*$^{Ku/Ku}$ Mutants

The altered position of the otocyst, relative to the hindbrain as well as the failure of endolymphatic duct formation, suggested that otocyst patterning might be affected by loss of *Zic2* function. Cells in the otic epithelium integrate multiple signals, especially from the SHH, WNT, and BMP pathways, leading to regionalized gene expression in the otic epithelium. We next looked at the expression of genes that are regulated by WNT, SHH, and BMP signaling and that are expressed in specific regions of the otic epithelium to determine if loss of *Zic2* function interfered with signal transduction by one or more pathways.

The *Pax2* transcription factor is one of the first genes expressed in the otic epithelium (Hutson et al., 1999) and its expression is positively regulated by SHH signaling but partially restricted by WNT and BMP signals from the dorsal hindbrain (Riccomagno et al., 2002, 2005). *Pax2* expression (Fig. 8) was relatively unchanged in the otic epithelium of the *Zic2*$^{Ku/Ku}$ mutants at E9.5 and E10.5 when compared to inner ears from *Zic2*$^{+/+}$ and *Zic2*$^{Ku/+}$ littermates (compare Figs. 8A,D and 8B,E, C,F). At a later stage of development (E12.5), *Pax2* expression was greatly reduced in the otic epithelium of the *Zic2*$^{Ku/Ku}$ mutants when compared to inner ears from *Zic2*$^{+/+}$ and *Zic2*$^{Ku/+}$ littermates (compare Fig. 8G and H, I). The *Pax2* expression pattern in mutant embryos suggested that the earliest events in otocyst patterning are unaltered by *Zic2* loss, but that the maintenance of expression of this key inner ear patterning gene *is* affected by *Zic2* loss.

We, therefore, examined the distribution of further genes known to be expressed in a regionalized manner within the developing otocyst in response to neurectoderm-derived signals.

The expression of the *Dlx5* transcription factor is negatively regulated by SHH signaling and positively regulated by WNT signaling (Riccomagno et al., 2002, 2005). The region of *Dlx5* expression in the otic epithelium of the *Zic2*$^{Ku/Ku}$ embryos remained associated with the cells in which it is normally found in the otocyst, although the otocyst itself is tilted laterally

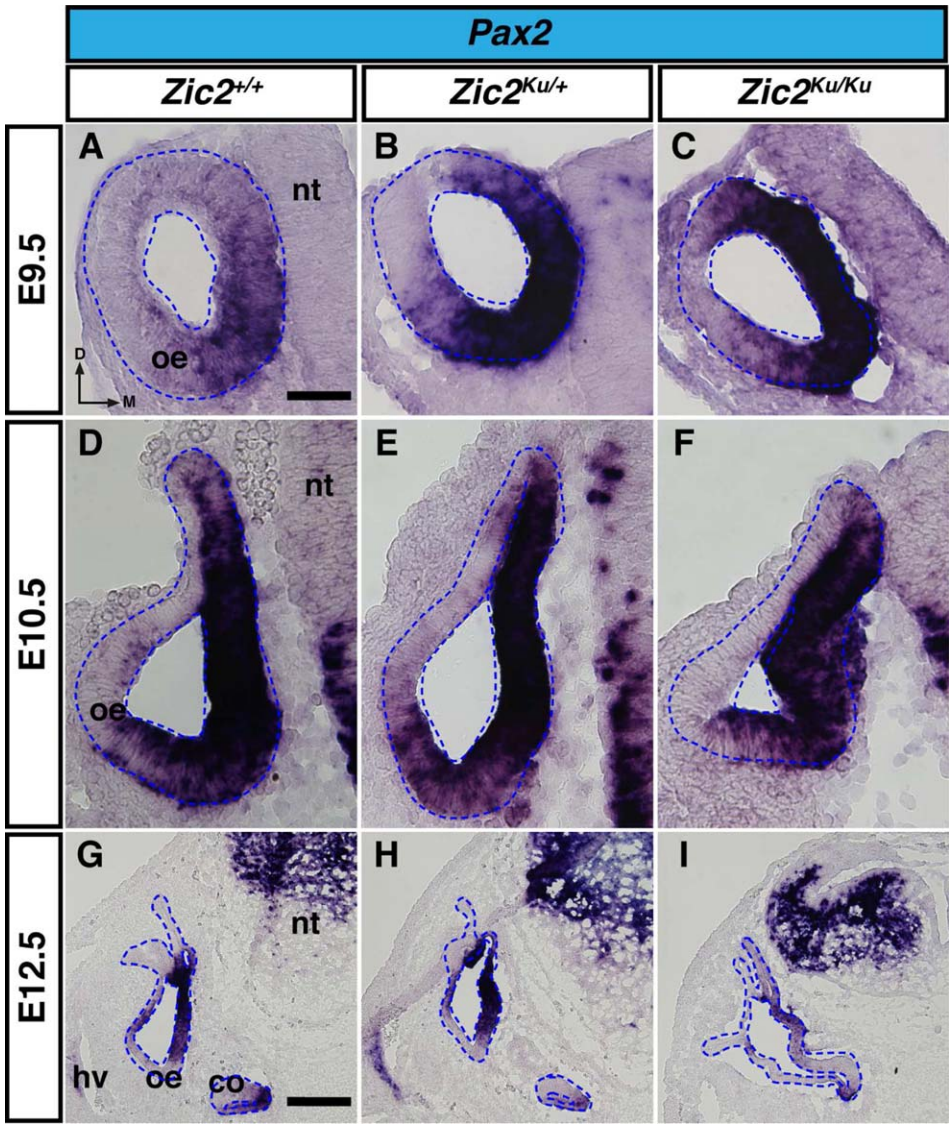

Fig. 8. Comparison of *Pax2* expression in the developing inner ear in the $Zic2^{Ku}$ mouse model. In situ hybridization using a probe for *Pax2* was performed on sections through the inner ear region of $Zic2^{+/+}$ (**A, D, G**), $Zic2^{Ku/+}$ (**B, E, H**), and $Zic2^{Ku/Ku}$ (**C, F, I**) embryos at E9.5 (A–C), E10.5 (D–F), and E12.5 (G–I). Blue dashed lines outline the otic epithelium. oe, otic epithelium; nt, neural tube; co, cochlea; hv, head vein; D, dorsal; M, medial. Scale bar in A = 50 μm (applies to A–F); scale bar in G = 200 μm (applies to G–I).

(compare Fig. 9C and 9A, B). The lack of a morphologically identifiable emerging endolymphatic duct and sac (ED/ES) is evident in this profoundly altered morphological landscape, in which the relationship of the developing inner ear to the affected/open NT is quite different from that in heterozygotes (compare Fig. 9A–C).

The regional expression of the *Gbx2* transcription factor is positively regulated by both SHH and WNT signaling within the domain that encompasses the presumptive endolymphatic duct cells (Riccomagno et al. 2002, 2005). The regional expression or extent of *Gbx2* transcripts in otocysts from $Zic2^{Ku/Ku}$ mutants, however, was much less than that seen in $Zic2^{+/+}$ and $Zic2^{Ku/+}$ inner ears at E10.5 (compare Fig. 9F and D, E), establishing this as the first detected molecular abnormality in mutant otocysts. Again, the lack of an emerging ED/ES was noted in the $Zic2^{Ku/Ku}$ mutant embryos.

Lfng is a SHH-responsive gene whose expression shifts in the absence of *Shh*. Although the region of expression of *Lfng* in the otic epithelium of $Zic2^{Ku/Ku}$ embryos (Fig. 9G–I) appeared to change relative to that found in $Zic2^{Ku/+}$ and $Zic2^{+/}$ embryos, it is possible this apparent change was due to the malformation of the neural tube and altered/missing outgrowth of the ED/ES from the dorsal portion of the otocyst. The open neural tube displaced the otocyst laterally, causing the region of *Lfng* expression to appear to have shifted laterally. If the otocyst were tilted medially back into its normal position relative to the D-V axis, the region of *Lfng* expression would be indistinguishable from that found in otocysts from wild type mice. *Lfng* expression also appears to be more extensive in the otocyst in $Zic2^{Ku/Ku}$ mice (compare Fig. 9I and 9G,H). However, since the outgrowth of the endolymphatic duct and sac is altered (either completely absent or severely delayed developmentally) in the ears of $Zic2^{Ku/Ku}$ mice (Fig. 3C), this apparent expansion of expression could be explained by alterations in the dorsal outgrowth of the otic epithelium.

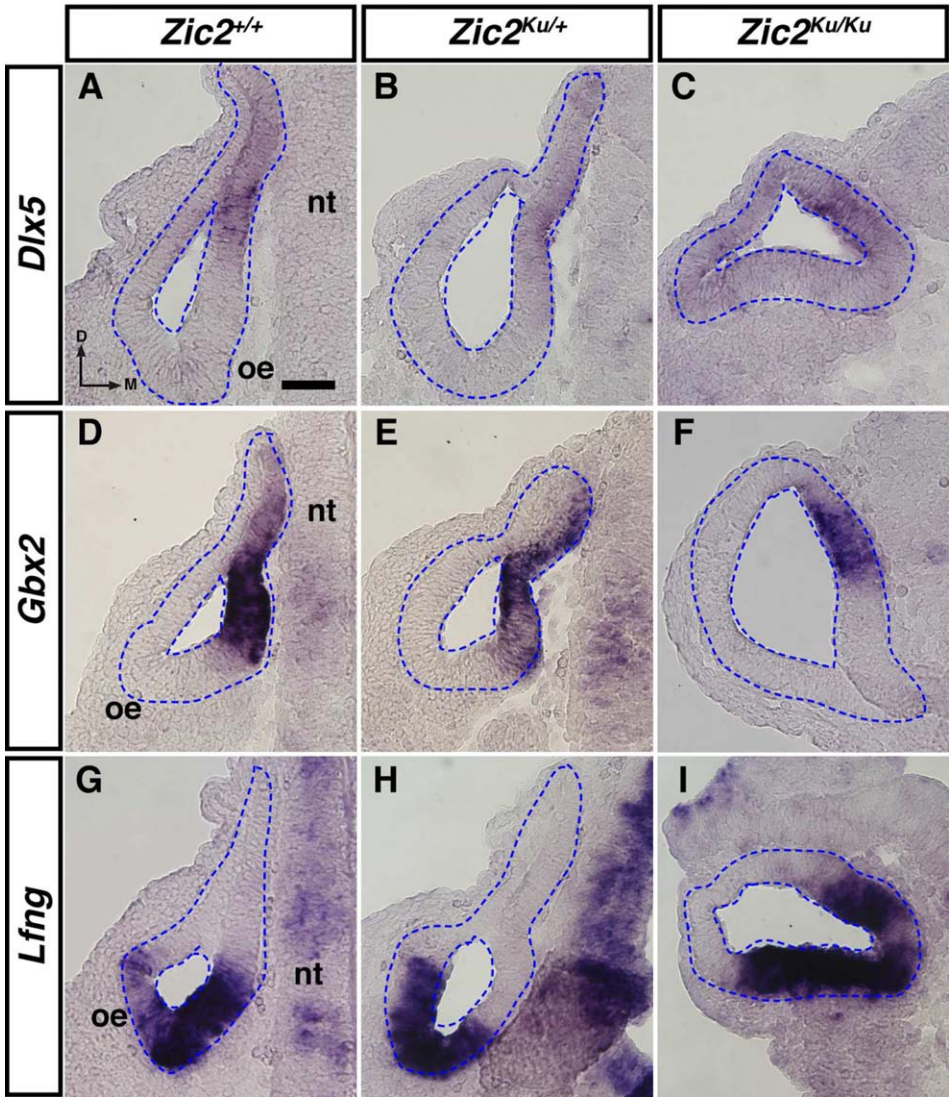

Fig. 9. Comparison of *Dlx5*, *Gbx2*, and *Lfng* expression in the developing inner ear at E10.5 in the *Zic2*^{Ku} mouse model. In situ hybridization using probes for *Dlx5* (**A–C**), *Gbx2* (**D–F**), and *Lfng* (**G–I**) were performed on sections through the inner ear region of *Zic2*$^{+/+}$ (A, D, G), *Zic2*$^{Ku/+}$ (B, E, H), and *Zic2*$^{Ku/Ku}$ (C, F, I) embryos. Blue dashed lines outline the otic epithelium. oe, otic epithelium; nt, neural tube; D, dorsal; M, medial. Scale bar in A = 50 μm (applies to A–I).

Expression of Mesenchymal Genes Is Relatively Unchanged in *Zic2*$^{Ku/Ku}$ Mutants

In *Zic2*$^{Ku/Ku}$ mutants, there is an increase in the distance between the neural tube and the otocyst, and this increase in distance corresponded to an increase in the number of cells filling the space between these two structures. We looked at the expression of *Tbx1* and *Brn4* to determine if these cells were periotic mesenchyme cells or regions of condensing cartilage as we had done in our earlier study (Chervenak et al., 2013). The changed position of the otocyst relative to the sources of WNT and SHH signals may have affected the expression of both *Tbx1* and *Brn4*, two genes that are regulated by WNT and SHH signaling (Riccomagno et al., 2002, 2005). *Tbx1* is normally expressed in the dorsolateral half of the otic epithelium and in the mesenchyme between the neural tube and otic epithelium, as well as in the mesenchyme adjacent to the ventral otic epithelium. This expression pattern was found in inner ears from *Zic2*$^{+/+}$, *Zic2*$^{Ku/+}$, and *Zic2*$^{Ku/Ku}$ embryos at both E9.5 and E10.5 and in *Zic2*$^{Ku/Ku}$ embryos; the cells found between the neural tube and the developing inner ear were *Tbx1*$^{+}$, indicating that these are periotic mesenchyme cells (data not shown). In mice with engineered *Tbx1* loss-of-function, neural fate is expanded and the VIIIth cranial ganglion rudiment (which would go on in WT animals to form both the auditory/spiral ganglion and the vestibular ganglion) is duplicated posteriorly (Raft et al., 2004). The inner ear in the *Tbx*-loss of function mice is hypoplastic with no vestibular apparatus or coiled cochlear duct. The authors (Raft et al., 2004) suggested that *Tbx1* could be a "selector gene" controlling neural and sensory organ fate specification in the otocyst. A *Tbx1* null homozygous mutation causes otocyst hypoplasia and arrest of inner ear morphogenesis (Jerome and Papaioannou, 2001; Vitelli et al., 2003). *Tbx1* heterozygosity is also associated with chronic otitis media (Liao et al., 2004). However, based on these limited experiments, it could not be determined whether the increase in periotic mesenchyme we observed was due to increased

proliferation of periotic mesenchyme cells or a result of periotic mesenchyme cells being displaced due to the severe morphological defects in these embryos. *Brn4* expression at E9.5 and E10.5 also appeared to be unchanged in the $Zic2^{Ku/Ku}$ mutants, indicating no apparent changes in the regions of condensing cartilage (data not shown).

Discussion

The Zic genes encode a family of transcription factors, which interact with a variety of signal transduction pathways, including the SHH, WNT, and BMP pathways that are known to be involved in inner ear development. Each of the Zic proteins is expressed in the POM during the early stages of inner ear development. Here we investigate for the first time whether mutation of the Zic genes impairs inner ear development. We find that combined loss of the *Zic1*/*Zic4* bi-gene has no apparent effect on inner ear development but that moderate or severe loss of *Zic2* function is associated with inner ear dysgenesis. This dysgenesis can be traced to the earliest stages of the otic morphogenesis because there is no evidence of endolymphatic duct initiation at E10.5 and decreased size of the developing inner ear is evident by E11.5. The initial patterning of the otocyst epithelium appears independent of *Zic2* function with the first molecular defects detected at E10.5.

Zic2 Acts Non-Cell-Autonomously to Influence Inner Ear Development

Either mild ($Zic2^{kd/kd}$) or severe ($Zic2^{Ku/Ku}$) loss of murine *Zic2* function results in significant defects in inner ear morphology. In the $Zic2^{kd/kd}$ inner ears, both dorsal (vestibular) and ventral (cochlea) structures are severely affected, notable by E13.5. Defects in the inner ears of $Zic2^{Ku/Ku}$ mice are seen earlier, starting at E11.5, and likely reflect the effect of further decreasing levels of Zic2 function. Inner ears from $Zic2^{Ku/Ku}$ mice exhibit either delayed or absent outgrowth of both the endolymphatic sac and endolymphatic and cochlear ducts, and are smaller than wild type ears along both the A-P (~60% of wild type size) and D-V axes (~50% of wild type size) at both E11.5 and E12.5 (Fig. 3). The mid-gestation demise of $Zic2^{Ku/Ku}$ embryos precludes direct comparison with $Zic2^{kd/kd}$ embryos past E12.5. It therefore remains unknown whether the more severe allele leads to different effects on inner ear development or accelerates the onset of the same defects seen in the $Zic2^{kd/kd}$ mice. Many other *Zic2*-associated phenotypes are semi-dominant (i.e., are more severe/have an earlier onset in the homozygous state) (Elms et al., 2003) and it is possible that the more severe loss-of-function in the $Zic2^{Ku/Ku}$ embryos accelerates the onset of the $Zic2^{kd/kd}$ defects.

During the initial stages of murine inner ear development, *Zic2* is expressed in the dorsal hindbrain and in the mesenchyme adjacent to the otic epithelium (Chervenak et al., 2013). *Zic2* expression in the mesenchyme expands in a dorsal to ventral wave between E9.5 and E11.5, with expression initially restricted to the dorsal and medial periotic mesenchyme at E9.5 (Chervenak et al., 2013). *Zic2*-expressing periotic mesenchyme cells completely surround the otic epithelium from earliest developmental times but *Zic2* is not expressed in the otic epithelium in any of the species examined (Chervenak et al., 2013). The expression data imply that *Zic2* acts in a non-cell-autonomous manner to influence inner ear morphogenesis.

Function of *Zic2* During Inner Ear Development

There are several possible mechanisms by which *Zic2* function may influence inner ear development. First, *Zic2* function may be required within the hindbrain neurectoderm to direct inner ear development. The importance of the hindbrain for inner ear development is evident from the analysis of mice with mutation of either *Hoxa1* or *Mafb* (aka *kreisler*) (Vazquez-Echeverria et al., 2008). Both *Hoxa1* and *Mafb* are transcription factors that are expressed in the hindbrain but not inner ear, but mutation of either is associated with inner ear defects that include absence of the endolymphatic duct. The abnormal inner ear development in these mutants is attributed in particular to defects in rhombomere 5 (r5), the region of the hindbrain adjacent to the developing otic placode.

The mechanism by which the hindbrain directs inner ear morphogenesis is not completely known, but loss of the *Gbx2* gene phenocopies many aspects of the Kreisler mutation, including the failure of endolymphatic duct development. *Gbx2* is a transcription factor expressed in the endolymphatic duct region of the otocyst and a likely downstream target of hindbrain signaling (Lin et al., 2005). The possibility that the inner ear dysmorphology results from loss of *Zic2* function in the neurectoderm is particularly enticing in view of the known disruption to hindbrain patterning in $Zic2^{Ku/Ku}$ embryos, in which the size of r5 is decreased (Elms et al., 2003) and the fact that altered *Gbx2* expression in the otocyst is the first molecular abnormality detected in the inner ear of $Zic2^{Ku/Ku}$ embryos (Fig 9).

A second possibility is that the defects in inner ear development are secondary to the neural tube defects found in *Zic2* mutants. These neural tube closure defects affect the positioning of the otocyst relative to the hindbrain (Fig 7), and thus may alter the "reach" of the WNT, BMP, and SHH signals from hindbrain to otocyst, resulting in altered patterning of the otocyst. Mutations in over 240 genes have been identified that lead to severe neural tube defects (Harris and Juriloff, 2007, 2010), but of these only a few, such as *Pax2*, show both inner ear and neural tube defects (Puschel et al., 1992; Torres et al., 1996). It, therefore, does not directly follow that neural tube defects prevent inner ear morphogenesis. In addition, both $Zic2^{kd/kd}$ and $Zic2^{Ku/Ku}$ mutants have severe neural tube defects (Nagai et al., 2000; Elms et al., 2003), but the severity of inner ear defects correlates with decreased *Zic2* function.

It is also possible that the inner ear defects in the *Zic2* mutants ($Zic2^{kd/kd}$ and $Zic2^{Ku/Ku}$) are a direct result of the loss of *Zic2* expression in the periotic mesenchyme. In this scenario, *Zic2* could act either to promote the mesenchymal-epithelial interactions crucial for inner ear development, or to relay the secreted signals from the neuroepithelium to the otic vesicle that drive both morphogenesis of the otic epithelium. The *Tbx1* transcription factor is expressed in both the otocyst and in the POM and deletion of *Tbx1* from the POM alone results in defects in cochlear duct outgrowth and coiling (Braunstein et al., 2009). Similarly, mice null for *Brn4*, a Pou domain transcription factor expressed in the POM but not otic vesicle, display a reduction in the number of turns of the cochlear duct (Phippard et al., 1999). Furthermore, neither the expression of *Tbx1* nor *Brn4* in the POM was altered in $Zic2^{Ku/Ku}$ embryos. Therefore, if *Zic2* is required in the POM for inner ear morphogenesis, it does not act upstream of these transcription factors. It is also possible that the hindbrain-derived neural crest is abnormal in *Zic2* mutant embryos and

contributes to the excess POM seen in some mutants. Our previous analysis of neural crest cell development in *Zic2*$^{Ku/Ku}$ embryos detected no abnormalities in the hindbrain derived crest suggesting this is an unlikely scenario (Elms et al., 2003). In the absence of a conditional allele of *Zic2* to enable tissue-specific inactivation of *Zic2*, it is difficult to distinguish whether *Zic2* expression is required in the neurectoderm, the POM, or both tissues.

Zic2 and Auditory and Vestibular Function

The mid-gestation lethality of *Zic2*$^{Ku/Ku}$ embryos precludes analysis of auditory and vestibular function in these animals. There is, however, evidence from other mouse models that experimentally induced alterations in otocyst morphogenesis can compromise inner ear function, even when hair and supporting cells are generated (Hatch et al., 2007; Nichols et al., 2008; Koo et al., 2009). Similarly, human genetic studies support the notion that stereotypic morphogenesis of the otocyst is necessary for normal auditory and vestibular function. For example, imaging reveals significant inner ear dysmorphologies in 30–40% of children with sensorineural hearing loss (Antonelli et al., 1999; Purcell et al., 2003). The work presented here extends the list of murine genes known to be required for correct otocyst morphogenesis. Furthermore, the ZIC2 protein is highly conserved between mouse and human and *Zic2* mutation in the mouse recapitulates the known human ZIC2 disease association of holoprosencephaly (Brown et al., 1998; Warr et al., 2008). It seems probable that ZIC2 loss-of-function in humans may also result in altered inner ear development and deficits in auditory and/or vestibular function.

The Loss of *Zic1* and *Zic4* May Be Compensated for by Other *Zic* Genes

Zic1 and *Zic4* have been shown to have redundant functions in cerebellar development, as loss of either *Zic1* or *Zic4* alone has a milder phenotype compared to a *Zic1*/*Zic4* double mutant (Aruga et al., 1998; Grinberg et al., 2004; Blank et al., 2011). When we analyzed the morphology of inner ears from *Zic1*$^{-/-}$; *Zic4*$^{-/-}$ embryos, we did not observe any obvious gross morphological defects in the size or shape of the developing inner ears through E15.5, the last stage examined. It is possible that *Zic1* and *Zic4* are involved in later development of the inner ear, such as in the development and maturation of the sensory patches. More likely, however, is that other *Zic* genes have redundant roles and can compensate for the loss of *Zic1* and *Zic4*, as the expression of *Zic1* and *Zic4* overlap in the dorso-medial periotic mesenchyme in a region in which both *Zic2* and *Zic3* are also expressed in the developing inner ear in both the chick and mouse (Chervenak et al., 2013).

Conclusions

Our experiments provide the first genetic evidence that the *Zic* genes are required for morphogenesis of the inner ear. Analysis of inner ear development in *Zic2*$^{Ku/Ku}$ mutants shows that the dysmorphology is presaged by molecular abnormality of the otic epithelium with the expression level and/or distribution of key transcription factors in the otic epithelium (*Pax2* and *Gbx2*) being altered by Zic2 loss-of-function. Experiments that distinguish whether there is a primary requirement for Zic2 function within the POM or whether earlier neurectoderm defects associated with Zic2 function are responsible for the inner ear development defects await the generation of a *Zic2* conditional allele. Given, however, that inner ear dysplasia is often associated with sensorineural hearing loss, *Zic2* should be considered as a candidate gene in ongoing efforts to identify the genetic basis of human auditory defects.

Experimental Procedures

Mouse Husbandry

The kumba (*Ku*) allele of *Zic2* was maintained by continuous backcross to 129/SvEv mice, and mice from backcross 10 or beyond were used for analysis. Mice were maintained in a light cycle of 12 hr light:12 hr dark, the midpoint of the dark cycle being 12 AM. For the production of staged embryos, 12 PM on the day of the appearance of the vaginal plug is designated E0.5. Pregnant females were sacrificed by cervical dislocation. The uterine horns containing the embryos were dissected out and placed in PBS with 10% FBS. Embryos were then dissected out of the surrounding maternal tissues and Reichert's membrane was removed. Embryos were fixed in 4% paraformaldehyde overnight, washed in 1X PBS (3 x 5 min), and then transferred to 30% sucrose in 1X PBS and rocked at 4°C overnight. Mice were genotyped by PCR screening of genomic DNA extracted from ear biopsy tissue (Thomsen et al., 2012) and embryos were genotyped using a fragment of extra embryonic tissue. Genomic DNA was extracted from embryonic tissue described previously (Arkell et al., 2001).

Embedding and Cryosectioning

Embryos were transferred through three progressive changes of OCT (TissueTek) to remove excess sucrose. The embryos were then transferred to embedding molds, covered with OCT, and oriented such that the anterior portion of the ear pointed down. The molds were then frozen on dry ice and stored at −80°C until sectioning. Transverse sections (12 μm) through the ear were cut using a Microm HM500M cryostat and collected on SuperFrost Plus slides (Fisher). Sections were air-dried on the slides at room temperature for at least 30 min, and then stored at −80°C.

In Situ Hybridization

In situ hybridization using digoxigenin-labeled antisense probes was performed on sections from *Zic2*$^{+/+}$, *Zic2*$^{Ku/+}$, and *Zic2*$^{Ku/Ku}$ embryos as previously described (Chervenak et al., 2013). A minimum of 2 embryos per genotype was analyzed for each probe. Antisense probes were generated by digesting plasmids containing the cDNA sequences of the genes of interest and then transcribing with the appropriate RNA polymerase. Images were acquired with an Olympus BX51 microscope equipped with an Olympus camera.

Paint-Filling of Inner Ears

Inner ears from *Zic2*^{kd}, *Zic2*^{kumba} and *Zic1*/*Zic4* mouse embryos were paint-filled using previously described protocols (Kiernan, 2006). A minimum of 2 ears per genotype was analyzed.

Imaging and Analysis of *Zic2*^{kumba} Embryos

Whole *Zic2*$^{+/+}$, *Zic2*$^{Ku/+}$, and *Zic2*$^{Ku/Ku}$ embryos and paint-filled inner ears from *Zic2*$^{+/+}$, *Zic2*$^{Ku/+}$, and *Zic2*$^{Ku/Ku}$ embryos

were imaged using a Nikon SMZ1500 stereomicroscope and fitted with a Nikon Digital Sight DS-Ri1 camera. The distance from the otocyst to the forelimb and the axial dimensions (anterior-posterior and dorsal-ventral) of the inner ear were measured using NIS Elements D 3.1 software.

Acknowledgments

The authors thank members of the Barald lab, Dr. Ben Allen, Dr. Sally Camper, Dr. David Kohrman, Dr. John Kuwada, and Dr. Yehoash Raphael, for helpful comments on the manuscript and advice on the experiments. We also thank Dr. Jun Aruga (RIKEN Institute) for the *Zic2*^{kd} embryos, Dr. Douglas Epstein (University of Pennsylvania) for the *Tbx1*, *Brn4*, *Dlx5*, and *Gbx2* probes, and Dr. Doris Wu (NIDCD) for the *Lfng* probe. This work was supported by NIH/NIDCD, 2 RO1 DC04184 and ARRA supplement (K.F.B.) and the Cellular and Molecular Biology (T32-GM007315), Regenerative Sciences (5T90DK070071-05), and Hearing, Balance, and Chemical Senses (5T32DC000011–32) training grants (A.P.C.).

References

Ali RG, Bellchambers HM, Arkell RM. 2012. Zinc fingers of the cerebellum (Zic): transcription factors and co-factors. Int J Biochem Cell Biol 44:2065–2068.

Antonelli PJ, Varela AE, Mancuso AA. 1999. Diagnostic yield of high-resolution computed tomography for pediatric sensorineural hearing loss. Laryngoscope 109:1642–1647.

Arkell RM, Cadman M, Marsland T, Southwell A, Thaung C, Davies JR, Clay Y, Beechey CV, Evans EP, Strivens MA, Brown SD, Denny P. 2001. Genetic, physical, and phenotypic characterization of the Del(13)Svea36H mouse. Mamm Genome 12:687–694.

Aruga J, Minowa O, Yaginuma H, Kuno J, Nagai T, Noda T, Mikoshiba K. 1998. Mouse Zic1 is involved in cerebellar development. J Neurosci 18:284–293.

Aruga J, Yokota N, Hashimoto M, Furuichi T, Fukuda M, Mikoshiba K. 1994. A novel zinc finger protein, zic, is involved in neurogenesis, especially in the cell lineage of cerebellar granule cells. J Neurochem 63:1880–1890.

Barratt KS, Glanville-Jones HC, Arkell RM. 2014. The Zic2 gene directs the formation and function of node cilia to control cardiac situs. Genesis 52:626–635.

Blank MC, Grinberg I, Aryee E, Laliberte C, Chizhikov VV, Henkelman RM, Millen KJ. 2011. Multiple developmental programs are altered by loss of Zic1 and Zic4 to cause Dandy-Walker malformation cerebellar pathogenesis. Development 138: 1207–1216.

Braunstein EM, Monks DC, Aggarwal VS, Arnold JS, Morrow BE. 2009. Tbx1 and Brn4 regulate retinoic acid metabolic genes during cochlear morphogenesis. BMC Dev Biol 9:31.

Brown L, Paraso M, Arkell R, Brown S. 2005. In vitro analysis of partial loss-of-function ZIC2 mutations in holoprosencephaly: alanine tract expansion modulates DNA binding and transactivation. Hum Mol Genet 14:411–420.

Brown SA, Warburton D, Brown LY, Yu CY, Roeder ER, Stengel-Rutkowski S, Hennekam RC, Muenke M. 1998. Holoprosencephaly due to mutations in ZIC2, a homologue of Drosophila odd-paired. Nat Genet 20:180–183.

Chervenak AP, Hakim I, Barald KF. 2013. Spatiotemporal expression of Zic genes during vertebrate inner ear development. Dev Dyn 242:897–908.

Ebert PJ, Timmer JR, Nakada Y, Helms AW, Parab PB, Liu Y, Hunsaker TL, Johnson JE. 2003. Zic1 represses Math1 expression via interactions with the Math1 enhancer and modulation of Math1 autoregulation. Development 130:1949–1959.

Elms P, Siggers P, Napper D, Greenfield A, Arkell R. 2003. Zic2 is required for neural crest formation and hindbrain patterning during mouse development. Dev Biol 264:391–406.

Elms P, Scurry A, Davies J, Willoughby C, Hacker T, Bogani D, Arkell R. 2004. Overlapping and distinct expression domains of Zic2 and Zic3 during mouse gastrulation. Gene Expr Patterns 4: 505–511.

Grinberg I, Millen KJ. 2005. The ZIC gene family in development and disease. Clin Genet 67:290–296.

Grinberg I, Northrup H, Ardinger H, Prasad C, Dobyns WB, Millen KJ. 2004. Heterozygous deletion of the linked genes ZIC1 and ZIC4 is involved in Dandy-Walker malformation. Nat Genet 36: 1053–1055.

Harris MJ, Juriloff DM. 2007. Mouse mutants with neural tube closure defects and their role in understanding human neural tube defects. Birth Defects Res A Clin Mol Teratol 79:187–210.

Harris MJ, Juriloff DM. 2010. An update to the list of mouse mutants with neural tube closure defects and advances toward a complete genetic perspective of neural tube closure. Birth Defects Res A Clin Mol Teratol 88:653–669.

Hatch EP, Noyes CA, Wang X, Wright TJ, Mansour SL. 2007. Fgf3 is required for dorsal patterning and morphogenesis of the inner ear epithelium. Development 134:3615–3625.

Houtmeyers R, Souopgui J, Tejpar S, Arkell R. 2013. The ZIC gene family encodes multi-functional proteins essential for patterning and morphogenesis. Cell Mol Life Sci 70:3791–3811.

Hutson MR, Lewis JE, Nguyen-Luu D, Lindberg KH, Barald KF. 1999. Expression of Pax2 and patterning of the chick inner ear. J Neurocytol 28:795–807.

Jerome LA, Papaioannou VE. 2001. DiGeorge syndrome phenotype in mice mutant for the T-box gene, Tbx1. Nat Genet 27:286–291.

Kiernan AE. 2006. The paintfill method as a tool for analyzing the three-dimensional structure of the inner ear. Brain Res 1091:270–276.

Koo SK, Hill JK, Hwang CH, Lin ZS, Millen KJ, Wu DK. 2009. Lmx1a maintains proper neurogenic, sensory, and non-sensory domains in the mammalian inner ear. Dev Biol 333:14–25.

Koyabu Y, Nakata K, Mizugishi K, Aruga J, Mikoshiba K. 2001. Physical and functional interactions between Zic and Gli proteins. J Biol Chem 276:6889–6892.

Liao J, Kochilas L, Nowotschin S, Arnold JS, Aggarwal VS, Epstein JA, Brown MC, Adams J, Morrow BE. 2004. Full spectrum of malformations in velo-cardio-facial syndrome/DiGeorge syndrome mouse models by altering Tbx1 dosage. Hum Mol Genet 13:1577–1585.

Lim LS, Hong FH, Kunarso G, Stanton LW. 2010. The pluripotency regulator Zic3 is a direct activator of the Nanog promoter in ESCs. Stem Cells 28:1961–1969.

Lin Z, Cantos R, Patente M, Wu DK. 2005. Gbx2 is required for the morphogenesis of the mouse inner ear: a downstream candidate of hindbrain signaling. Development 132:2309–2318.

Mizugishi K, Aruga J, Nakata K, Mikoshiba K. 2001. Molecular properties of Zic proteins as transcriptional regulators and their relationship to GLI proteins. J Biol Chem 276:2180–2188.

Mizugishi K, Hatayama M, Tohmonda T, Ogawa M, Inoue T, Mikoshiba K, Aruga J. 2004. Myogenic repressor I-mfa interferes with the function of Zic family proteins. Biochem Biophys Res Commun 320:233–240.

Nagai T, Aruga J, Minowa O, Sugimoto T, Ohno Y, Noda T, Mikoshiba K. 2000. Zic2 regulates the kinetics of neurulation. Proc Natl Acad Sci USA 97:1618–1623.

Nichols DH, Pauley S, Jahan I, Beisel KW, Millen KJ, Fritzsch B. 2008. Lmx1a is required for segregation of sensory epithelia and normal ear histogenesis and morphogenesis. Cell Tissue Res 334:339–358.

Nyholm MK, Wu SF, Dorsky RI, Grinblat Y. 2007. The zebrafish zic2a-zic5 gene pair acts downstream of canonical Wnt signaling to control cell proliferation in the developing tectum. Development 134:735–746.

Pan H, Gustafsson MK, Aruga J, Tiedken JJ, Chen JC, Emerson Jr. CP. 2011. A role for Zic1 and Zic2 in Myf5 regulation and somite myogenesis. Dev Biol 351:120–127.

Phippard D, Lu L, Lee D, Saunders JC, Crenshaw 3rd EB. 1999. Targeted mutagenesis of the POU-domain gene Brn4/Pou3f4 causes developmental defects in the inner ear. J Neurosci 19: 5980–5989.

Pourebrahim R, Houtmeyers R, Ghogomu S, Janssens S, Thelie A, Tran AT, Langenberg T, Vleminckx K, Bellefroid E, Cassiman JJ,

Tejpar S. 2011. Transcription factor Zic2 inhibits Wnt/beta-catenin protein signaling. J Biol Chem 286:37732–37740.
Purcell D, Johnson J, Fischbein N, Lalwani AK. 2003. Establishment of normative cochlear and vestibular measurements to aid in the diagnosis of inner ear malformations. Otolaryngol Head Neck Surg 128:78–87.
Puschel AW, Westerfield M, Dressler GR. 1992. Comparative analysis of Pax-2 protein distributions during neurulation in mice and zebrafish. Mech Dev 38:197–208.
Raft S, Nowotschin S, Liao J, Morrow BE. 2004. Suppression of neural fate and control of inner ear morphogenesis by Tbx1. Development 131:1801–1812.
Riccomagno MM, Martinu L, Mulheisen M, Wu DK, Epstein DJ. 2002. Specification of the mammalian cochlea is dependent on Sonic hedgehog. Genes Dev 16:2365–2378.
Riccomagno MM, Takada S, Epstein DJ. 2005. Wnt-dependent regulation of inner ear morphogenesis is balanced by the opposing and supporting roles of Shh. Genes Dev 19:1612–1623.
Rohr KB, Schulte-Merker S, Tautz D. 1999. Zebrafish zic1 expression in brain and somites is affected by BMP and hedgehog signalling. Mech Dev 85:147–159.
Sakurada T, Mima K, Kurisaki A, Sugino H, Yamauchi T. 2005. Neuronal cell type-specific promoter of the alpha CaM kinase II gene is activated by Zic2, a Zic family zinc finger protein. Neurosci Res 53:323–330.
Salero E, Perez-Sen R, Aruga J, Gimenez C, Zafra F. 2001. Transcription factors Zic1 and Zic2 bind and transactivate the apolipoprotein E gene promoter. J Biol Chem 276:1881–1888.
Thomsen N, Ali RG, Ahmed JN, Arkell RM. 2012. High resolution melt analysis (HRMA); a viable alternative to agarose gel electrophoresis for mouse genotyping. PloS One 7:e45252.
Torres M, Gomez-Pardo E, Gruss P. 1996. Pax2 contributes to inner ear patterning and optic nerve trajectory. Development 122:3381–3391.
Vazquez-Echeverria C, Dominguez-Frutos E, Charnay P, Schimmang T, Pujades C. 2008. Analysis of mouse kreisler mutants reveals new roles of hindbrain-derived signals in the establishment of the otic neurogenic domain. Dev Biol 322: 167–178.
Vitelli F, Viola A, Morishima M, Pramparo T, Baldini A, Lindsay E. 2003. TBX1 is required for inner ear morphogenesis. Hum Mol Genet 12:2041–2048.
Warr, N., N. Powles-Glover, A. Chappell, J. Robson, D. Norris and R. M. Arkell 2008. Zic2-associated holoprosencephaly is caused by a transient defect in the organizer region during gastrulation. Hum Mol Genet 17:2986–2996.
Yang Y, Hwang CK, Junn E, Lee G, Mouradian MM. 2000. ZIC2 and Sp3 repress Sp1-induced activation of the human D1A dopamine receptor gene. J Biol Chem 275: 38863–38869.